2-12-2010

Organization, Structure, and Assembly of alpha-Carboxysomes Determined by Electron Cryotomography of Intact Cells

Cristina V. Iancu
California Institute of Technology

Dylan M. Morris
California Institute of Technology

Zhicheng Dou
University of Southern Mississippi

Sabine Heinhorst
University of Southern Mississippi, sabine.heinhorst@usm.edu

Gordon C. Cannon
University of Southern Mississippi, Gordon.Cannon@usm.edu

See next page for additional authors

Published in final edited form as:
J Mol Biol. 2010 February 12; 396(1): 105–117. doi:10.1016/j.jmb.2009.11.019.

Organization, Structure, and Assembly of α-Carboxysomes Determined by Electron Cryotomography of Intact Cells

Cristina V. Iancu[1,4,#], **Dylan M. Morris**[1,#], **Zhicheng Dou**[3,5], **Sabine Heinhorst**[3], **Gordon C. Cannon**[3], and **Grant J. Jensen**[1,2,*]

[1]Division of Biology, California Institute of Technology, Pasadena, CA 91125, USA

[2]Howard Hughes Medical Institute, California Institute of Technology, Pasadena, CA 91125, USA.

[3]Department of Chemistry and Biochemistry, The University of Southern Mississippi, Hattiesburg, MS 39406, USA.

Abstract

Carboxysomes are polyhedral inclusion bodies that play a key role in autotrophic metabolism in many bacteria. Using electron cryotomography, we examined carboxysomes in their native states within intact cells of three chemolithoautotrophic bacteria. We found that carboxysomes generally cluster into distinct groups within the cytoplasm, often in the immediate vicinity of polyphosphate granules, and a regular lattice of density frequently connects granules to nearby carboxysomes. Small granular bodies were also seen within carboxysomes. These observations suggest a functional relationship between carboxysomes and polyphosphate granules. Carboxysomes exhibited greater size, shape, and compositional variability in cells than in purified preparations. Finally, we observed carboxysomes in various stages of assembly, as well as filamentous structures that we attribute to misassembled shell protein. Surprisingly, no more than one partial carboxysome was ever observed per cell. Based on these observations, we propose a model for carboxysome assembly in which the shell and the internal RuBisCO lattice form simultaneously, likely guided by specific interactions between shell proteins and RuBisCOs.

Keywords

H. neapolitanus; bacterial microcompartment; carboxysome; cryo-EM; electron tomography

Introduction

Bacterial microcompartments are proteinaceous, polyhedral bodies that sequester particular enzymes within a thin protein shell.[1] By concentrating enzymes and substrates in the same

*To whom correspondence should be addressed: 1200 E. California Blvd., Pasadena, CA 91125, 626-395-8827 (phone), 626-395-5730 (fax), Jensen@caltech.edu..

[4]Present address: Department of Biochemistry and Molecular Biology, Rosalind Franklin University, The Chicago Medical School, North Chicago, IL 60064, USA

[5]Present address: Department of Microbiology and Immunology, University of Michigan School of Medicine, Ann Arbor, MI 48109, USA.

[#]These authors contributed equally.

space, microcompartments may enhance enzymatic activity, sequester volatile intermediates, and/or isolate enzymes from competitive inhibitors. The best characterized microcompartments are the carboxysomes found in all cyanobacteria and many chemoautotrophs.[2] The chemoautotrophic sulfur-oxidizing gammaproteobacterium *Halothiobacillus neapolitanus* has served as the model system for many investigations of α-carboxysomes, which are distinguished from β-carboxysomes by genetic architecture, shell composition, and the form of enzyme they encapsulate.[3]

The α-carboxysomes of *H. neapolitanus* self-assemble from ten polypeptides, eight of which are associated with the shell. The interior of the carboxysome is filled with the CO_2-fixing enzyme ribulose-1,5-bisphosphate carboxylase/oxygenase (RuBisCO), an inefficient enzyme that is vital to autotrophic metabolism.[4] A carboxysome shell-associated carbonic anhydrase5 provides the carboxysome-encapsulated RuBisCO with its substrate, CO_2 and, in combination with the partial impermeability of the carboxysome shell to CO_2,[6; 7] contributes to the catalytic advantage RuBisCO derives from being sequestered within the microcompartment. Most, if not all carboxysome gene mutants that form organelles compromised in structure and/or function are unable to grow efficiently at ambient CO_2 levels or do not survive at all unless cultured in CO_2-supplemented air. [6; 7; 8; 9; (reviewed in 10)

The crystal structures of CsoS1A, one of the three main α-carboxysome shell polypeptides, and of the minor shell constituent CsoS4A (formerly OrfA), have suggested an initial model of the carboxysome shell.[11; 12] A monolayer of tightly apposed CsoS1 hexamers is believed to form the facets of the icosahedral carboxysomes while pentamers of CsoS4A are thought to occupy the vertices. The structure of the α-carboxysomal carbonic anhydrase CsoSCA has also been solved.13 The exact location of this protein within the carboxysome is unknown, but biochemical evidence suggests that the enzyme is tightly associated with the interior of the carboxysome shell.7

Carboxysomes have been the subject of much electron microscopy.(e.g. 14; 15; 16; 17) More recently, purified α-carboxysomes from *H. neapolitanus*[18] and from the cyanobacterium *Synechococcus* WH8102[19] were examined by high-resolution electron cryotomography (ECT). These studies confirmed that carboxysomes are regular icosahedra, but unlike typical icosahedral viruses, exhibit a range of sizes. Schmid and colleagues speculated that differences in carboxysome sizes could be due to differing arrangements of shell proteins; Iancu et al. thought this unlikely and attributed size heterogeneity to potentially different T numbers (differences in the total number of shell proteins). Within the carboxysomes, RuBisCOs were found to be arranged in several concentric layers, with an estimated half located in the layer immediately adjacent to the shell, but no evidence for contacts between RuBisCOs and the shell proteins was found.[19]

While these studies elucidated the structure of purified carboxysomes, because the function of carboxysomes seems to be to sequester and organize certain reactions within the cell, understanding their position within and interactions with the rest of the cell is central. Recently, α-carboxysomes within intact cells of the cyanobacterium *Prochlorococcus* were visualized by ECT.[20] Here we used ECT to characterize α-carboxysomes within intact cells of *H. neapolitanus* as well as two other chemolithoautotrophic proteobacteria, *Thiomonas intermedia* and *Thiomicrospira crunogena*. We observed features relating to the organization, structure, and assembly of carboxysomes common to all three organisms. The most salient of these findings were novel structural associations linking carboxysomes and polyphosphate (polyP) granules, suggesting a functional relationship between these two ultrastructures. Within cells we observed carboxysomes in various stages of assembly. These observations suggest a model for carboxysome assembly in which the shell and the RuBisCO lattice form

simultaneously, potentially guided by specific interactions between shell proteins and RuBisCOs.

Results and Discussion

One hundred fifty-three tomograms were recorded of intact *H. neapolitanus* cells, which were typically rod-shaped, 0.5 μm wide, and approximately 1.5 μm long (though cell lengths varied as would be expected from unsynchronized cells, Fig. 1a). Many interesting structures were seen, including physical associations between carboxysomes and polyP granules, oddly shaped and irregular carboxysomes, partial carboxysomes, and cytoplasmic filaments. In order to determine whether these features were specific to *H. neapolitanus*, we also examined 20 and 14 cells (respectively) of two other chemoautotrophic sulfur-oxidizing proteobacteria, *T. intermedia* and *T. crunogena*. Cells of *T. intermedia* appeared ovoid to rod-shaped and similar in length to cells of *H. neapolitanus*, though slightly wider (Fig. 1b). Cells of *T. crunogena* were distinguished by their unique helical shapes (Fig. 1c). Because similar structures were also observed in these organisms, they are likely general features of chemolithoautotrophic sulfur oxidizers.

Organization of carboxysomes

In chemostat-grown *H. neapolitanus*, the number of carboxysomes per cell varied from 4 to 18, with an average of 10 per cell. The number of carboxysomes per cell in *T. intermedia* was higher (17), likely because these cells were imaged soon after transfer from heterotrophic to autotrophic growth conditions, which is known to rapidly induce carboxysome formation.[21] Cells of chemostat-grown *T. crunogena* exhibited a much greater variance in the number of carboxysomes per cell than the other two organisms, ranging from 5 to 80 or more. The number of carboxysomes per cell directly correlated with cell cycle and cell size. That is, elongated cells approaching division possessed greater numbers of carboxysomes than smaller cells. Furthermore, dividing cells contained strikingly similar numbers of carboxysomes within each nascent daughter cell (Fig. S1). In 17 out of 19 dividing cells, carboxysomes were as evenly segregated as possible, suggesting that some active mechanism might partition them.

In 98% of *H. neapolitanus* cells, carboxysomes were clustered together in groups of three or more, either by themselves (Fig. 2a) or around dark, electron-dense bodies (Fig. 2b). In only three cells were carboxysomes found dispersed throughout the cells with no apparent clustering (Fig. 2c). Carboxysome clustering appeared most pronounced in cells of *T. intermedia* (Fig. 1b), although this might simply be due to the larger numbers of carboxysomes present in these cells. In *T. crunogena* cells containing large numbers of carboxysomes, grouping was also readily apparent (Fig. S5a).

Grouping of β-carboxysomes was noted previously in the cyanobacterium *Anabaena* PCC 7119.[17] A recent ECT study of strains of another cyanobacterium, *Prochlorococcus*, found that the α-carboxysomes of those cells also cluster into groups within the cytoplasm.[20] This observation led the authors to suggest that such clustering might facilitate carbon fixation by allowing CO_2 leaked out of any carboxysome to be fixed by another in the group.[20] Carboxysomes may cluster simply because their components are synthesized in a single location within the cell, or some other mechanism may be involved such as the entropic effects of macromolecular crowding.[22]

Association of carboxysomes with polyP granules

On average, cells of *H. neapolitanus* contained two dark, electron-dense bodies within the cytoplasm. These dark bodies were also observed in cells of *T. intermedia* and *T. crunogena*. We used electron energy loss spectroscopy (EELS) to show that these bodies were enriched in

phosphorous relative to the surrounding cytoplasm (Figs. 3 and S3). Recently, Borgnia and colleagues used similar techniques to assign as polyP granules the dark bodies observed in cells of *Bdellovibrio bacteriovorus*.[23] Additionally, *H. neapolitanus* cells grown under phosphate limitation demonstrated either a significant reduction in the volume of these granular bodies or their complete disappearance. For these reasons, we propose that the dark bodies observed in *H. neapolitanus* cells are indeed polyP granules. In further support of this assignment, the *H. neapolitanus* genome (NC_013422.1) contains genes encoding enzymes responsible for polyP synthesis and hydrolysis. While similar EELS experiments were not performed on cells of *T. intermedia* or *T. crunogena*, given the structural and metabolic similarities between these bacteria and *H. neapolitanus*, it is likely that the electron-dense bodies present in these cells are polyP granules as well. In support of this conclusion, we note that the genomes of *T. crunogena*[24] and *T. intermedia* (unpublished) both also possess the key necessary genes.

In all three organisms, the association of carboxysomes with polyP granules was clear and consistent. In 96% of *H. neapolitanus* cells containing these granules, clusters of carboxysomes were found surrounding them, with an average of 2.5 carboxysomes (40% of the total in these cells) directly abutting each granule (Fig. 4). The polyP granules were typically spherical; in *H. neapolitanus*, they ranged in diameter from 40-200 nm, although smaller granules were sometimes also observed. Intriguingly, the polyP granules often exhibited indentations (Fig. 4b) or sharp and distinct facets (Fig. 4c) along their interfaces with carboxysomes.

Interesting patterns of density were often observed in the regions between the polyP granules and the adjacent carboxysomes. Figure 5 highlights two such patterns, which appear to be novel structural features physically linking carboxysomes to polyP granules. Thirty-seven percent of cells containing polyP granules presented ordered lattices. Ninety-four percent of these structures connected granules with neighboring carboxysomes, although in three cells we observed lattices emanating from granules with no carboxysomes nearby. The surfaces of the polyP granules often appeared faceted in the regions connected to the lattices (Fig. 5a), but lattices protruding out of spherical granules were also observed (Fig. 5b). The periodicity of the lattice was approximately 6.3 nm.

Strings of density linking polyP granules to nearby carboxysomes were seen in 24% of the cells containing polyP granules (Fig. 5c). Gaps in the carboxysome shell were sometimes observed near these strings (Fig. 5d). While it is unclear what constitutes the lattices and strings, an intriguing possibility is that they are oligomers of polyphosphate kinase, which forms filaments in the presence of ATP.[25] Regardless, these physical connections between carboxysomes and polyP granules suggest a significant functional relationship.

Internal granules

In addition to the physical connections between polyP granules and carboxysomes, evidence that there may be a functional relationship between the two ultrastructures came from the observation of dark granular structures within many carboxysomes (Figs. 6 and S6). In *H. neapolitanus* cells, 26% of all carboxysomes presented these internal high-density granules; in three extreme cells, 90% of carboxysomes contained these granules. Carboxysomes possessing internal granules were observed in 77% of all *H. neapolitanus* cells, and were present in all three bacteria examined. Within the carboxysomes of *T. crunogena*, in addition to granules, in 3 out of 14 cells we observed high-density fibers that spanned the entire diameter of the carboxysome (Fig. 6, panels 11-12).

The internal granules varied in size, shape, and position within the carboxysome. The higher electron scattering of these granules as compared to neighboring RuBisCOs suggests they are not composed of protein. More likely they are aggregations of small molecules. Visually, these

internal granules appear to have a similar density to the cytoplasmic polyP granules described above. We attempted to use the EELS technique to analyze these granules, but their small size prevented us from making reliable determinations. A slight correlation (r = 0.76) was observed between the volume of a cell's polyP granules and the percent of the cell's carboxysomes that contained internal granules, hinting that there may be some relationship between the two. Furthermore, cells limited for phosphate or thiosulfate had a significantly lower number of carboxysomes with internal granules (5% and 8% of total carboxysomes, respectively) than cells not limited for these nutrients (31% of total carboxysomes).

While the composition of these internal granules remains unclear, we propose that they are polyP. In support of this interpretation, Tang and colleagues used energy dispersive X-ray spectroscopy to show that carboxysomes of the cyanobacterium *Synechococcus leopoliensis* contain granules composed of inorganic phosphate and calcium.[26] This composition is similar to that of cytoplasmic polyP granules.[27] An alternative explanation for the presence of the internal granules is that they are aggregates of the phosphorylated substrates and/or products of the RuBisCO reaction.

Size, shape, and compositional variability of cellular carboxysomes

The size, shape, and composition of cellular carboxysomes varied, especially in *T. crunogena*. Besides the canonical icosahedral shape, we found carboxysomes that were irregular or elongated (Fig. 7, a-d) (as observed previously14). Additionally, carboxysomes of significantly different sizes were often found to co-exist within the same cells (Fig. 7e). Extremely elongated carboxysomes were observed in cells of both *T. intermedia* (Fig. S4b) and *T. crunogena* (Fig. 1c), sometimes spanning the entire cell. While most carboxysomes contained densely packed RuBisCOs, two intact *H. neapolitanus* carboxysomes contained large gaps within their internal lattices of RuBisCOs (Fig. S2, panel 1). Similar electron-translucent gaps within β-carboxysomes were reported in previous analyses of cyanobacteria.[17; 28] The presence of carboxysomes containing loosely packed RuBisCOs is intriguing, given that such loose packing would likely reduce the rate of carbon fixation that these carboxysomes could achieve.[29] It seems likely that loose packing arises from rapid formation of carboxysomes, as RuBisCOs within the carboxysomes of cells of *T. intermedia* switched to autotrophic growth media were more often loosely packed (Fig. S2, panels 2-6).

Comparable uniformity of in vitro *carboxysomes*

Along with the cellular carboxysomes, we recorded 26 tilt-series of carboxysomes purified from *H. neapolitanus* containing a total of 203 intact carboxysomes. In contrast to carboxysomes observed within cells, which varied widely in size and shape, and as observed previously,[18; 19] purified carboxysomes were mostly regular icosahedra and none contained internal granules (Fig. 8) (though three carboxysomes contained internal structures larger than RuBisCO, but of similar density, most likely corresponding to aggregated protein). Purification therefore likely enriches for well-formed, structurally robust carboxysomes, while selecting against internal granules. Eighty-two carboxysomes were manually segmented in 3-D to allow accurate measurement. These varied in diameter from 116 to 169 nm, with an average of 134 +/− 8 nm. These results are roughly consistent with those reported previously by Schmid et al. (average diameter of ~100 nm),[18] considering Schmid et al. measured radial density distributions of spherically averaged carboxysomes (corresponding approximately to inscribed spheres), while we measured the lengths of carboxysome edges directly (corresponding to circumscribed spheres, which for regular icosahedra are 26% larger). The relative standard deviation of icosahedral edges observed here varied from 5.5 to 17.2%.

In addition to intact carboxysomes, several broken carboxysomes were also observed. Because rows of RuBisCOs were seen packed against broken carboxysome shells, there must be some

interaction that links them. Menon et al. recently suggested that such interactions might explain why α-carboxysomes fail to compartmentalize non-carboxysomal RuBisCO.[9]

Partial carboxysomes

Many cells contained partial carboxysomes (54% in *H. neapolitanus*), but there was never more than one partial carboxysome per cell. As ECT provides only static information, we cannot be sure whether these partial carboxysomes were in the process of assembly or degradation at the time of freezing. Nevertheless because many were observed in cells grown under conditions known to induce carboxysome formation,[30] and because all the cultures were actively growing, we believe the majority of partial carboxysomes were assembling. Partial carboxysomes spanning the range of likely assembly intermediates were observed (Figs. 9 and S7). Multiple layers of RuBisCOs aligned along the inner surface of some of the shells (e.g. Fig. 9, panels 5 and 10), suggesting that RuBisCOs are attracted to both the shell and each other. While this would predict that RuBisCOs should also aggregate away from carboxysome shells, we did not see any such aggregates. RuBisCO aggregates have been observed, however, in electron micrographs of high concentrations of purified RuBisCOs.[28]

The geometries of nascent carboxysome shells were strikingly variable: some had sharp and distinct vertices (e.g. Fig. 9, panels 1, 6 and 12) while others were smooth and gently curved (e.g. Fig. 9, panels 7, 9, and especially 10). How interactions between the carboxysome shell proteins might give rise to both rounded and faceted carboxysomes remains unclear, but the presence of isolated vertices and facets show they can form independently of any interactions with RuBisCOs. Indeed, empty carboxysome shells were recently seen in an *H. neapolitanus* mutant lacking RuBisCO.[9] No empty shells were observed in the wild-type cells examined here.

These results argue against models of carboxysome assembly where the shell forms first and then RuBisCOs are transported inside.[31] Another early model proposed that RuBisCOs self-assemble into an icosahedral core that provides a template for later shell assembly.[28] Our observation of carboxysomes with loosely packed RuBisCOs and gaps within the internal RuBisCO lattice, as well as the absence of RuBisCO aggregates, make this mechanism seem unlikely. This model is also discounted by the fact that in purified carboxysomes, the innermost layers of RuBisCOs are less well-ordered than the outermost.[19]

Instead our observations suggest that RuBisCOs pack within carboxysomes as the shell assembles. As shell facets grow and vertices form, specific interactions between shell proteins and RuBisCOs likely cause the latter to pack along the inner surface of the nascent shell. Indeed complexes of RuBisCO with shell proteins of β-carboxysomes were recently identified, lending support to this idea.[32; 33] The ordering of RuBisCOs into multiple layers prior to complete encapsulation suggests that further interactions exist between RuBisCOs. Because we never observed more than one partial carboxysome per cell, shell nucleation must be rate-limiting.

Filamentous structures

Parallel and twisted bundles of filaments were observed in 39% and 3% of *H. neapolitanus* cells, respectively. While 3 out of 5 of the twisted filaments were observed in close proximity to carboxysomes (Fig. 10a), the parallel bundles were, without exception, located close to the cell membrane (Fig. 10b-e). The periodicity of some of these parallel bundles was detectable, which we measured to be 6.9 nm (Fig. 10d). This value is close to the 6.7 nm spacing between adjacent hexamers in the crystal structure of the CsoS1A shell protein.[11] In some cases, the parallel bundles formed tubes, and were flanked by rows of densities similar in size and shape to RuBisCOs (Fig. 10e).

Cytoplasmic filaments have been identified in many diverse bacteria,[34] but the composition and function of the majority of these filaments remains unknown. Carboxysome-associated tubular filaments were reported previously in cells of the cyanobacterium *Anabaena*.[35] Tubular filaments were previously described in electron microscopy of thin sections of *Salmonella enterica* when a homolog of the carboxysome shell proteins, PduA, was overproduced.[36] Tubular filaments were also observed in a strain of *E. coli* engineered to possess the propanediol microcompartment from *Citrobacter freundii* when PduA was overexpressed.[37] Furthermore, Kerfeld and colleagues found that the hexamers of β-carboxysome shell proteins crystallized into tightly packed sheets and strips, with inter-hexamer spacings of ~7 nm.[38] Thus while it is not certain, at least some of the parallel bundles we observed here are likely misassembled shell protein, sometimes holding rows of RuBisCOs.

Speculations on the functional relevance of carboxysome/polyP associations

As described above, in all three organisms, carboxysomes were generally found clustered into groups within the cytoplasm, most often associated with polyP granules. These associations included indentations and facets on the surfaces of the granules directly abutting neighboring carboxysomes, lattices and strings physically linking carboxysomes and granules, and (likely) phosphate-rich granules within carboxysomes. We conclude that there must be an important functional relationship between carboxysomes and polyP granules, but what it might be is unclear. PolyP granules have been proposed to serve in bacterial cells as storage reserves for elemental phosphorous or divalent cations such as Mg^{2+} and Ca^{2+}, transient and spatially-localized sources of energy, buffers against alkalinity, and mediators of stress responses.[27; 39; 40; 41]

It is unknown in what form polyP is stored within these granules. Chains of polyP range from tens to hundreds of phosphate residues long and have no inherent tertiary structure.42 PolyP is formed by the transfer of a phosphate group from ATP to the growing polyP chain, and under conditions of ATP limitation, polyP can be used to synthesize ATP from ADP or AMP.[27] PolyP may also substitute for ATP as the phosphate donor in some enzyme-catalyzed phosphorylation reactions, either directly or via the action of an exopolyphosphatase (Ppx).[40] Intriguingly, in the genome of *H. neapolitanus* (NC_013422.1), the gene encoding Ppx precedes a cluster of genes encoding three enzymes of the Calvin cycle, including two that immediately follow the RuBisCO reaction, phosphoglycerate kinase (*pgk*) and glyceraldehyde-3- phosphate dehydrogenase (*gpd*). As the Pgk reaction requires a phosphate donor, the polyP granules may be supplying either phosphate or energy to Pgk or one of the many other phosphorylation reactions within the Calvin cycle that are likely occurring in the vicinity.

The proposed role of polyP granules in pH buffering suggests an alternative explanation.[27] While carbonic anhydrase releases a hydroxide ion for each molecule of CO_2 produced, the RuBisCO carboxylation reaction releases a corresponding proton. Although direct measurements of the pH inside carboxysomes have not been made, if the carbonic anhydrase produces saturating concentrations of CO_2, there should always be a net excess of hydroxide ions compared to protons. Under such alkaline conditions, hydrolysis of the polyP chain (which releases protons) could restore a neutral pH in the region.

If the internal granules are in fact composed of polyP, they might similarly help buffer the pH within the carboxysome. Alternatively, they might promote RuBisCO activation. It has been shown that RuBisCO of the cyanobacterium *Synechocystis* PCC6803 is activated by inorganic phosphate in a manner similar to the action of the RuBisCO activase of higher plants.[43; 44; 45] The internal polyP granules might provide a ready source of inorganic phosphate within the carboxysome to maintain an activated RuBisCO population. PolyP is also known to bind and store divalent cations such as Mg^{2+}.[27] As Mg^{2+} is a necessary cofactor for the RuBisCO carboxylation reaction, it is possible that internal polyP granules function as localized stores

of this important ion. It is important to note, however, that internal granules were present in only about a quarter of all carboxysomes.

Conclusion

In order to fully understand carboxysomes, we must understand their relationship to the rest of the cell. By imaging carboxysomes in 3-D within intact cells in a near-native state, we found that cellular carboxysomes exhibited greater variability than purified carboxysomes in terms of internal organization, size, and shape. Reconstructions of assembly intermediates *in vivo* revealed that RuBisCOs pack into carboxysomes as their shells are forming. Finally, carboxysomes *in vivo* were often physically associated with polyP granules and contained smaller granules, raising important questions about the functional relationship between these two structures.

Materials and Methods

Bacterial strains and culture conditions

Halothiobacillus neapolitanus C2 ATCC 23641 and *Thiomicrospira crunogena* XCL-2 were grown in a chemostat at a dilution rate of 0.08 h^{-1} in air supplemented with 5% CO_2 as described previously.[46; 47] *H. neapolitanus* cells were grown under different CO_2 (5%, 0.04%, or 0.01%), thiosulfate, or phosphate concentrations. In the phosphate limitation experiment, the potassium phosphate in the medium was replaced with 50 mM HEPES. *Thiomonas intermedia* K12 was maintained as a batch culture in heterotrophic or mixotrophic medium.[21] For the carbon downshift experiment, the bacteria were pelleted by centrifugation and resuspended in autotrophic medium.

H. neapolitanus carboxysome purification

Carboxysomes were purified according to So et al.[5] and brought to a final concentration of 1 mg/ml in 10 mM Tris pH 8.0.

Cryo-sample preparation

Bacterial cells—Pellet from 5-10 ml cell culture centrifuged at 3000 g for 7 minutes was resuspended in 50 μl cell culture and combined with the pellet of 450 μl of BSA-treated 10-nm colloidal gold.48 Three microliters of the mixture was applied to each grid (Quantifoil Micro Tools, Jena, Germany) before plunge freezing into ethane:propane,[49] using either a Vitrobot (FEI Company, Hillsboro, OR; manual application, blot time 1-2 s, blot offset −1 or −2 mm) or a gravity plunger.

Purified *H. neapolitanus* carboxysomes—Ten microliters of sample (1 mg/ml in 10 mM Tris pH 8.0) were combined with the pellet of 50 μl of 10-nm colloidal gold, previously centrifuged for 5 mins at 18000 g on a microfuge. The mixture was applied on holey carbon grids (Quantifoil Micro Tools, Jena, Germany) under 95% or higher humidity, using a Vitrobot and the following parameters: manual application of 3 μl/ grid, 2s blot time and −2 mm blot offset.

Electron Microscopy

Standard EM tilt-series were collected on a 300 kV FEG “G2 Polara” TEM electron cryomicroscope, equipped with a 2 × 2 k Gatan Ultrascan CCD camera or a lens-coupled 4 × 4 k Ultracam (Gatan, Pleasanton, CA). Energy-filtered (20 eV slit width) image series were acquired with the UCSF tomography package.[50] Cellular tomograms were collected from −60 to + 60°, with an angular step of 1°, total dose ranging from 120 to 190 e/$Å^2$, defocus values

of 12 μm, at pixel sizes on the specimen of 1.259 or 0.961 nm. Tilt series for the purified carboxysomes were collected from −69 or 70 to + 69 or 70°, with angular steps of 1, 1.5 or 2°, total doses of 110, 120, 140, or 150 e/Å^2 defocus values ranging from 4 to 12 μm, at pixel sizes of 0.46, 0.56, or 0.67 nm. A total of 153, 20, 14, and 26 tilt series were collected for *H. neapolitanus*, *T. intermedia*, *T. crunogena* cells, and purified *H. neapolitanus* carboxysomes, respectively.

Cryo-electron spectroscopic imaging

Data collection for phosphorus elemental map for *H. neapolitanus* cells was done as described previously[51] with the following modifications. For 15 target cells, data collection strategy involved: acquisition of a tit series (+/− 60° tilt range, 1° step size, 12 μm defocus, 70 e/Å^2 total dose) first acquired, followed by recording of post-edge, first and second pre-edge images (each of 20-35 e/Å^2) with the 20 eV energy filter slit positioned at 142, 117, and 97 eV, respectively. Data collection for eleven additional cells excluded the initial tilt series. Background on-edge modeling was done as previously described.[51] Background subtraction and three-window elemental map computation were produced with custom-made programs, after initial relative alignment of images using Bsoft.[52]

Data processing and analysis

Three-dimensional reconstructions were generated with IMOD.[53] Segmentation of the outer shells of purified *H. neapolitanus* carboxysomes was done with Amira (Mercury Computer Systems), after initial extraction of carboxysomes from tomograms using Bsoft.[52] For each carboxysome, the icosahedral edges were measured to estimate the size of carboxysomes and the deviation from regular icosahedra.19

Supplementary Material

Refer to Web version on PubMed Central for supplementary material.

Acknowledgments

We are indebted to Dr. Raj Menon for culturing *T. crunogena* cells, Dr. Eric Williams for providing purified *H. neapolitanus* carboxysomes and initial batches of *H. neapolitanus* cells, Dr. H. Jane Ding for computational help with generation of phosphorus elemental maps, Dr. William F. Tivol for technical assistance in setting up the spectroscopic imaging experiments, and Dr. Elizabeth R. Wright for freezing grids and imaging several *T. intermedia* cells. This work was supported in part by NIH grants R01 AI067548 and P50 GM082545 to GJJ, DOE grant DE-FG02-04ER63785 to GJJ, NSF grant MCB-0818680 to GCC and SH, the Beckman Institute at Caltech, and gifts to Caltech from the Gordon and Betty Moore Foundation and Agouron Institute.

References

1. Cheng S, Liu Y, Crowley CS, Yeates TO, Bobik TA. Bacterial microcompartments: their properties and paradoxes. Bioessays 2008;30:1084–95. [PubMed: 18937343]
2. Yeates T, Kerfeld C, Heinhorst S, Cannon GC, Shively JM. Protein-based organelles in bacteria: carboxysomes and related microcompartments. Nat Rev Microbiol 2008;6:681–691. [PubMed: 18679172]
3. Badger MR, Price GD. CO2 concentrating mechanisms in cyanobacteria: molecular components, their diversity and evolution. Journal of Experimental Botany 2003;54:609–622. [PubMed: 12554704]
4. Spreitzer RJ, Salvucci ME. Rubisco: structure, regulatory interactions, and possibilities for a better enzyme. Annual review of plant biology 2002;53:449–75.
5. So AK, Espie GS, Williams EB, Shively JM, Heinhorst S, Cannon GC. A novel evolutionary lineage of carbonic anhydrase (epsilon class) is a component of the carboxysome shell. Journal of Bacteriology 2004;186:623–30. [PubMed: 14729686]

6. Heinhorst S, Williams EB, Cai F, Murin CD, Shively JM, Cannon GC. Characterization of the carboxysomal carbonic anhydrase CsoSCA from Halothiobacillus neapolitanus. J Bacteriol 2006;188:8087–94. [PubMed: 17012396]
7. Dou Z, Heinhorst S, Williams EB, Murin CD, Shively JM, Cannon GC. CO2 fixation kinetics of Halothiobacillus neapolitanus mutant carboxysomes lacking carbonic anhydrase suggest the shell acts as a diffusional barrier for CO2. J Biol Chem 2008;283:10377–84. [PubMed: 18258595]
8. Baker S, Jin S, Aldrich H, Howard G, Shively J. Insertion mutation of the form I cbbL gene encoding ribulose bisphosphate carboxylase/oxygenase (RuBisCO) in Thiobacillus neapolitanus results in expression of form II RuBisCO, loss of carboxysomes, and an increased CO2 requirement for growth. Journal of Bacteriology 1998;180:4133–4139. [PubMed: 9696760]
9. Menon BB, Dou Z, Heinhorst S, Shively JM, Cannon GC. Halothiobacillus neapolitanus carboxysomes sequester heterologous and chimeric RubisCO species. PLoS ONE 2008;3:e3570. [PubMed: 18974784]
10. Price GD, Sultemeyer D, Klughammer B, Ludwig M, Badger M. The functioning of the CO2 concentrating mechanism in several cyanobacterial strains: a review of general physiological characteristics, genes, proteins, and recent advances. Canadian Journal of Botany 1998;76:973–1002.
11. Tsai Y, Sawaya MR, Cannon GC, Cai F, Williams EB, Heinhorst S, Kerfeld CA, Yeates TO. Structural Analysis of CsoS1A and the Protein Shell of the Halothiobacillus neapolitanus Carboxysome. PLoS Biol 2007;5:e144. [PubMed: 17518518]
12. Tanaka S, Kerfeld CA, Sawaya MR, Cai F, Heinhorst S, Cannon GC, Yeates TO. Atomic-Level Models of the Bacterial Carboxysome Shell. Science 2008;319:1083. [PubMed: 18292340]
13. Sawaya MR, Cannon GC, Heinhorst S, Tanaka S, Williams EB, Yeates TO, Kerfeld CA. The structure of beta-carbonic anhydrase from the carboxysomal shell reveals a distinct subclass with one active site for the price of two. J Biol Chem 2006;281:7546–55. [PubMed: 16407248]
14. Shively JM, Ball FL, Kline BW. Electron microscopy of the carboxysomes (polyhedral bodies) of Thiobacillus neapolitanus. Journal of Bacteriology 1973;116:1405–11. [PubMed: 4127632]
15. Jensen TE. Cyanobacterial cell inclusions of irregular occurrence: systematic and evolutionary implications. Cytobios 1984;39:35–62.
16. Holthuijzen YA, Breemen J, Konings WN, Bruggen E. Electron microscopic studies of carboxysomes of Thiobacillus neapolitanus. Arch Microbiol 1986;144:258–262.
17. Orús MI, Rodríguez-Buey ML, Marco E, Fernández-Valiente E. Changes in carboxysome structure and grouping and in photosynthetic affinity for inorganic carbon in Anabaena strain PCC 7119 (Cyanophyta) in response to modification of CO2 and Na+ supply. Plant Cell Physiol 2001;42:46–53. [PubMed: 11158443]
18. Schmid MF, Paredes AM, Khant HA, Soyer F, Aldrich HC, Chiu W, Shively JM. Structure of Halothiobacillus neapolitanus carboxysomes by cryo-electron tomography. J Mol Biol 2006;364:526–35. [PubMed: 17028023]
19. Iancu CV, Ding HJ, Morris DM, Dias DP, Gonzales AD, Martino A, Jensen GJ. The structure of isolated Synechococcus strain WH8102 carboxysomes as revealed by electron cryotomography. J Mol Biol 2007;372:764–773. [PubMed: 17669419]
20. Ting CS, Hsieh C, Sundararaman S, Mannella C, Marko M. Cryo-electron tomography reveals the comparative three-dimensional architecture of prochlorococcus, a globally important marine cyanobacterium. J Bacteriol 2007;189:4485–93. [PubMed: 17449628]
21. Purohit K, Mcfadden BA, Shaykh MM. D-Ribulose-1,5-bisphosphate carboxylase and polyhedral inclusion bodies in Thiobacillus intermedius. Journal of Bacteriology 1976;127:516–22. [PubMed: 179979]
22. Zhou HX, Rivas G, Minton AP. Macromolecular crowding and confinement: biochemical, biophysical, and potential physiological consequences. Annual review of biophysics 2008;37:375–97.
23. Borgnia MJ, Subramaniam S, Milne JLS. Three-Dimensional Imaging of the Highly Bent Architecture of Bdellovibrio bacteriovorus by Using Cryo-Electron Tomography. Journal of Bacteriology 2008;190:2588. [PubMed: 18203829]
24. Scott K, Sievert S, Abril F, Ball L, Barrett C, Blake R, Boller A, Chain PS, Clark J, Davis C, Detter C, Do K, Dobrinski K, Faza B, Fitzpatrick K, Freyermuth S, Harmer T, Hauser L, Hügler M, Kerfeld

CA, Klotz M, Kong W, Land M, Lapidus A, Larimer F, Longo D, Lucas S, Malfatti S, Massey S, Martin D, Mccuddin Z, Meyer F, Moore J, Ocampo L, Paul J, Paulsen IT, Reep D, Ren Q, Ross R, Sato P, Thomas P, Tinkham L, Zeruth G. The genome of deep-sea vent chemolithoautotroph Thiomicrospira crunogena XCL-2. PLoS Biol 2006;4:e383. [PubMed: 17105352]

25. Fraley CD, Rashid MH, Lee SSK, Gottschalk R, Harrison J, Wood PJ, Brown MRW, Kornberg A. A polyphosphate kinase 1 (ppk1) mutant of Pseudomonas aeruginosa exhibits multiple ultrastructural and functional defects. PNAS 2007;104:3526–3531. [PubMed: 17360677]
26. Tang M, Jensen TE, Corpe WA. The occurrence of polyphosphate bodies in polyhedral bodies (carboxysomes) in Synechococcus leopoliensis (Cyanophyceae). Microbios 1995;81:59–66.
27. Kornberg A, Rao NN, Ault-Riche D. Inorganic Polyphosphate: A Molecule of Many Functions. Annual Reviews in Biochemistry 1999;68:89–125.
28. Orus MI, Rodriguez ML, Martinez F, Marco E. Biogenesis and Ultrastructure of Carboxysomes from Wild Type and Mutants of Synechococcus sp. Strain PCC 7942. Plant Physiology 1995;107:1159–1166. [PubMed: 12228422]
29. Lizana L, Konkoli Z, Bauer B, Jesorka A, Orwar O. Controlling chemistry by geometry in nanoscale systems. Annual review of physical chemistry 2009;60:449–68.
30. Beudeker R, Cannon G, Kuenen JG, Shively J. Relations between D-ribulose-1, 5-bisphosphate carboxylase, carboxysomes and CO 2 fixing capacity in the obligate chemolithotroph Thiobacillus neapolitanus grown under different limitations in the chemostat. Arch Microbiol 1980;124:185–189.
31. Price GD, Badger MR. Evidence for the role of carboxysomes in the cyanobacterial CO2-concentrating mechanism. Can J Bot 1991;69:963–973.
32. Long BM, Badger MR, Whitney SM, Price GD. Analysis of Carboxysomes from Synechococcus PCC7942 Reveals Multiple Rubisco Complexes with Carboxysomal Proteins CcmM and CcaA. J Biol Chem 2007;282:29323–35. [PubMed: 17675289]
33. Cot SS, So AK, Espie GS. A multiprotein bicarbonate dehydration complex essential to carboxysome function in cyanobacteria. J Bacteriol 2008;190:936–45. [PubMed: 17993516]
34. Li Z, Jensen GJ. Electron cryotomography: a new view into microbial ultrastructure. Curr Opin Microbiol 2009;12:333–340. [PubMed: 19427259]
35. Jensen TE, Ayala RP. The Fine Structure of a Microplate-Microtubule Array, Microfilaments and Polyhedral Body Associated Microtubules in Several Species of Anabaena. Arch Microbiol 1976;111:1–6. [PubMed: 828027]
36. Havemann GD, Sampson EM, Bobik TA. PduA is a shell protein of polyhedral organelles involved in coenzyme B(12)-dependent degradation of 1,2-propanediol in Salmonella enterica serovar typhimurium LT2. Journal of Bacteriology 2002;184:1253–61. [PubMed: 11844753]
37. Parsons JB, Dinesh SD, Deery E, Leech HK, Brindley AA, Heldt D, Frank S, Smales CM, Lünsdorf H, Rambach A, Gass MH, Bleloch A, McClean KJ, Munro AW, Rigby SE, Warren MJ, Prentice MB. Biochemical and structural insights into bacterial organelle form and biogenesis. J Biol Chem 2008;283:14366–75. [PubMed: 18332146]
38. Kerfeld CA, Sawaya MR, Tanaka S, Nguyen CV, Phillips M, Beeby M, Yeates TO. Protein structures forming the shell of primitive bacterial organelles. Science 2005;309:936–8. [PubMed: 16081736]
39. Kornberg A. Inorganic polyphosphate: toward making a forgotten polymer unforgettable. Journal of Bacteriology 1995;177:491–6. [PubMed: 7836277]
40. Kulaev I, Kulakovskaya T. Polyphosphate and phosphate pump. Annu Rev Microbiol 2000;54:709–34. [PubMed: 11018142]
41. Seufferheld MJ, Alvarez HM, Farias ME. Role of polyphosphates in microbial adaptation to extreme environments. Appl Environ Microbiol 2008;74:5867–74. [PubMed: 18708516]
42. Brown MR, Kornberg A. The long and short of it -- polyphosphate, PPK and bacterial survival. Trends Biochem Sci 2008;33:284–90. [PubMed: 18487048]
43. Marcus Y, Gurevitz M. Activation of cyanobacterial RuBP-carboxylase/oxygenase is facilitated by inorganic phosphate via two independent mechanisms. European Journal of Biochemistry 2000;267:5995–6003. [PubMed: 10998060]
44. Marcus Y, Altman-Gueta H, Finkler A, Gurevitz M. Mutagenesis at two distinct phosphate-binding sites unravels their differential roles in regulation of Rubisco activation and catalysis. Journal of Bacteriology 2005;187:4222–8. [PubMed: 15937184]

45. Andersson I. Catalysis and regulation in Rubisco. Journal of Experimental Botany 2008;59:1555–68. [PubMed: 18417482]

46. Cannon G, Shively J. Characterization of a homogenous preparation of carboxysomes from Thiobacillus neapolitanus. Arch Microbiol 1983;134:52–59.

47. Dobrinski K, Longo D, Scott K. The carbon-concentrating mechanism of the hydrothermal vent chemolithoautotroph Thiomicrospira crunogena. Journal of Bacteriology 2005;187:5761–6. [PubMed: 16077123]

48. Iancu C, Tivol W, Schooler J, Dias D, Henderson G, Murphy G, Wright E, Li Z, Yu Z, Briegel A. Electron cryotomography sample preparation using the Vitrobot. Nature protocols 2006;1:2813–2819.

49. Tivol W, Briegel A, Jensen G. An Improved Cryogen for Plunge Freezing. MAM 2008;14:375–379.

50. Zheng Q, Braunfeld M, Sedat J, Agard D. An improved strategy for automated electron microscopic tomography. Journal of Structural Biology 2004;147:91–101. [PubMed: 15193638]

51. Comolli LR, Kundmann M, Downing KH. Characterization of intact subcellular bodies in whole bacteria by cryo-electron tomography and spectroscopic imaging. Journal of Microscopy 2006;223:40–52. [PubMed: 16872430]

52. Heymann JB, Belnap DM. Bsoft: image processing and molecular modeling for electron microscopy. Journal of Structural Biology 2007;157:3–18. [PubMed: 17011211]

53. Kremer J, Mastronarde D, McIntosh JR. Computer visualization of three-dimensional image data using IMOD. Journal of Structural Biology 1996;116:71–76. [PubMed: 8742726]

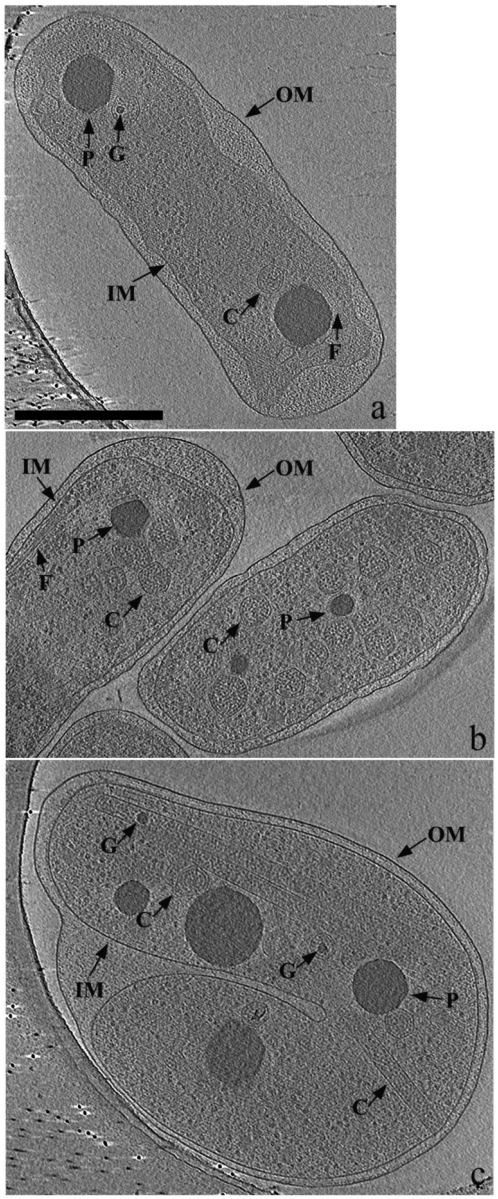

Figure 1.

Overview of the three organisms examined: a) *H. neapolitanus*; b) *T. intermedia*; c) *T. crunogena*. A wealth of structural features can be seen including high-density granules (P), carboxysomes (C), internal granules and fibers (G), and filamentous structures (F). Also visible are the inner (IM) and outer membranes (OM). All images representing cells here and throughout are tomographic slices (usually 12-nm thick). Scale bar is 500 nm.

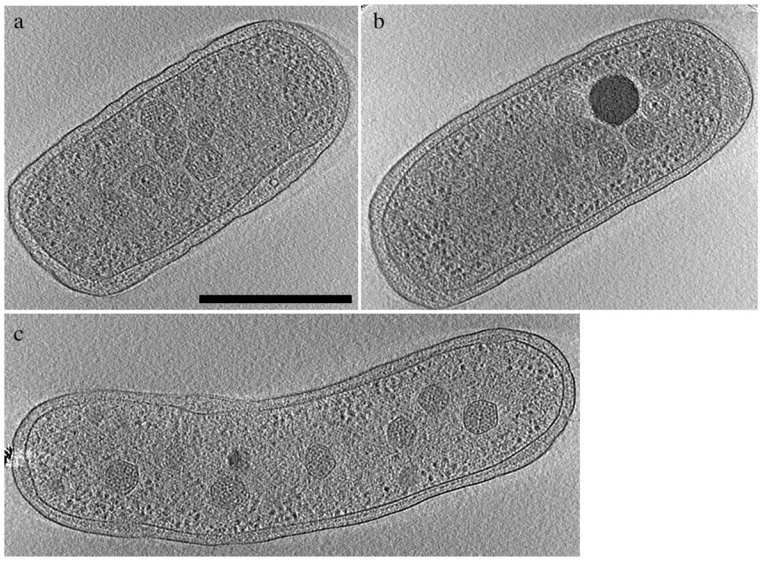

Figure 2.
Organization of carboxysomes in *H. neapolitanus* cells: a) group of carboxysomes clustered together near the center of a cell; b) carboxysomes packed around an electron-dense granule; c) carboxysomes dispersed throughout the cell. Scale bar is 500 nm.

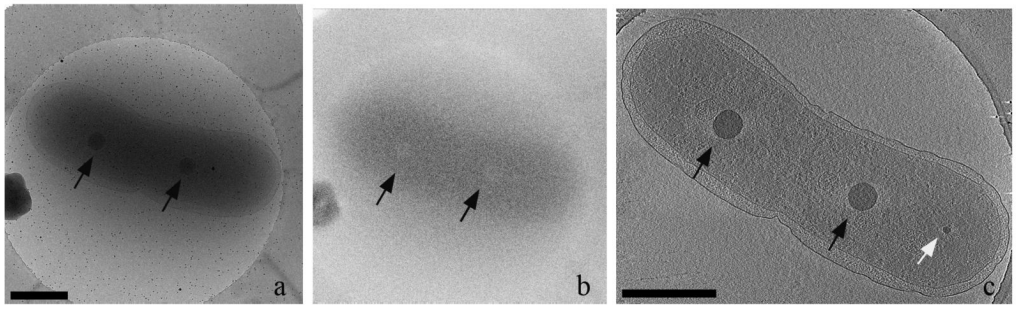

Figure 3.
Elemental analysis of dense granules. The figure shows three images of the same *H. neapolitanus* cell: a) zero-loss 2-D projection image; b) 2-D projection electron energy loss spectrographic image focused on phosphorous; c) slice through the corresponding tomogram. The black arrows in a) and c) highlight dense granules; the black arrows in b) highlight regions rich in phosphorous. The white arrow in c) highlights an internal granule too small to be detected by the elemental map. Scale bars are 500 nm.

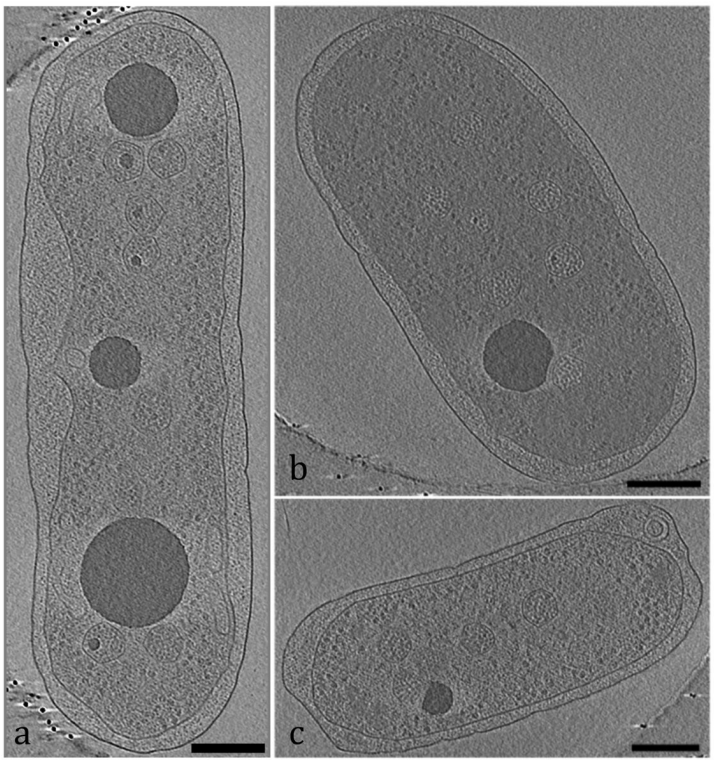

Figure 4.
Associations of carboxysomes with polyP granules: a) *H. neapolitanus* cell, showing close association between carboxysomes and granules (note the string of density between the topmost granule and the adjacent carboxysomes, as well as the densities within the carboxysomes, which resemble the densities of the polyP granules); b) *H. neapolitanus* cell, showing indentation of the polyP granule surface where it abuts a carboxysome (note the line of density between the indented face of the granule and the adjacent carboxysome); c) *H. neapolitanus* cell, showing faceted granule abutting carboxysome (note the lattice emanating from this facet). Scale bars are 200 nm.

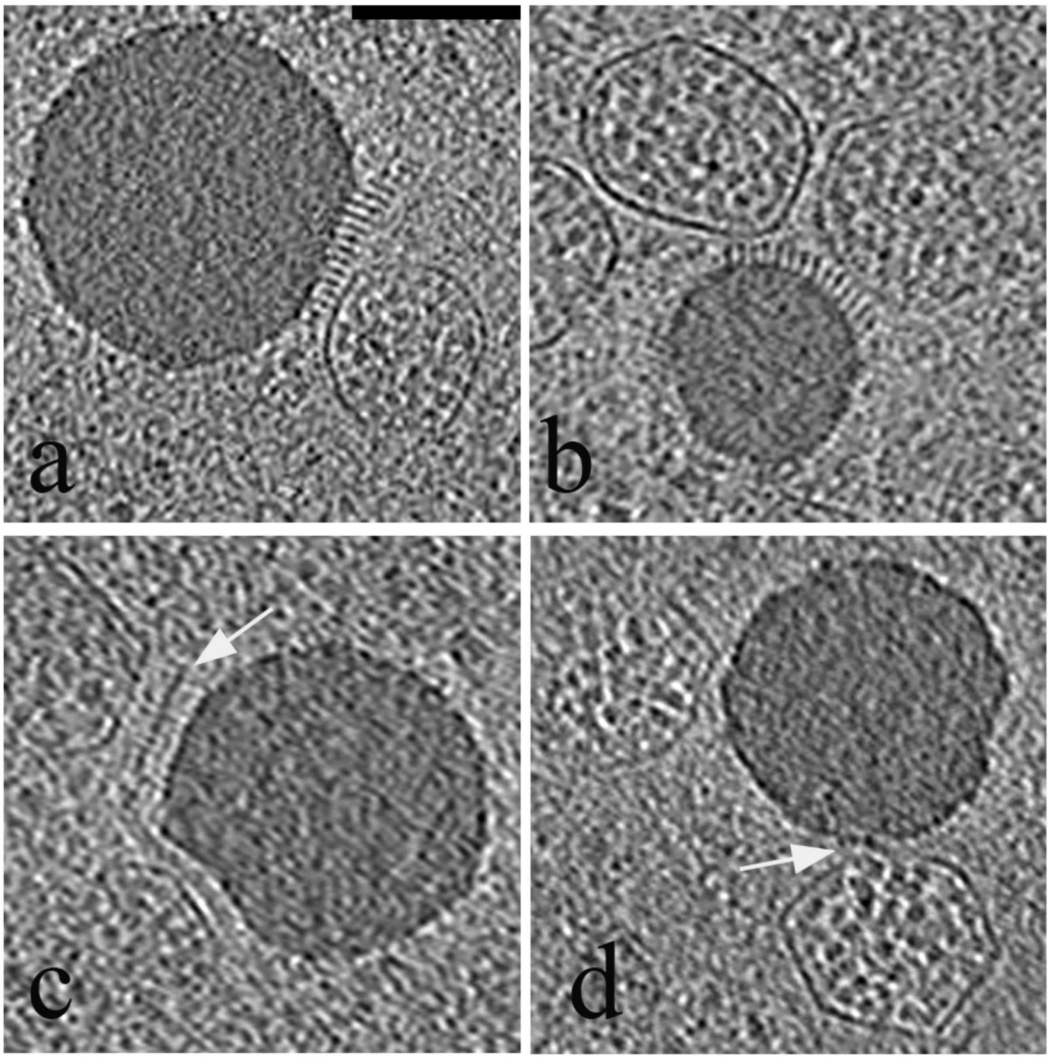

Figure 5.
Lattices and strings: a) lattice protruding from a polyP granule and toward a neighboring carboxysome in an *H. neapolitanus* cell; b) lattice emanating out of the curved surface of a polyP granule and toward two adjacent carboxysomes in a *T. intermedia* cell; c) string between an indented polyP granule and the neighboring carboxysome; d) string connecting a polyP granule to an adjacent carboxysome (note the indentation in the polyP granule and the apparent gap in the carboxysome surface where the string is attached). Scale bar is 100 nm.

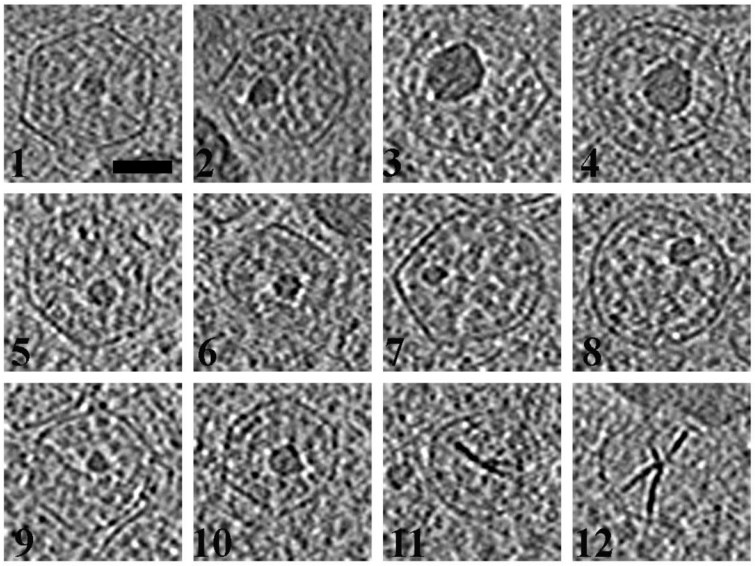

Figure 6.
Dense granules and fibers within carboxysomes. Panels 1-4 show increasing sizes of internal granules in *H. neapolitanus* carboxysomes. Panels 5-8 show *T. intermedia* carboxysomes and panels 9-12 show *T. crunogena* carboxysomes. Panels 11 and 12 illustrate the dense fibers observed inside carboxysomes of *T. crunogena*. Scale bar is 50 nm.

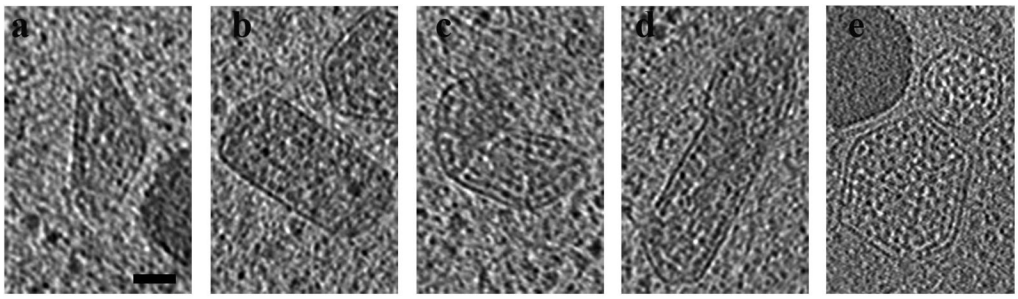

Figure 7.
Size and shape variability of cellular carboxysomes: a)-d) irregular carboxysomes; e) two adjacent icosahedral carboxysomes of different sizes. Panels a), b), c), and e) are from cells of *H. neapolitanus*. Panel d) is from a cell of *T. intermedia*. Scale bar is 50 nm.

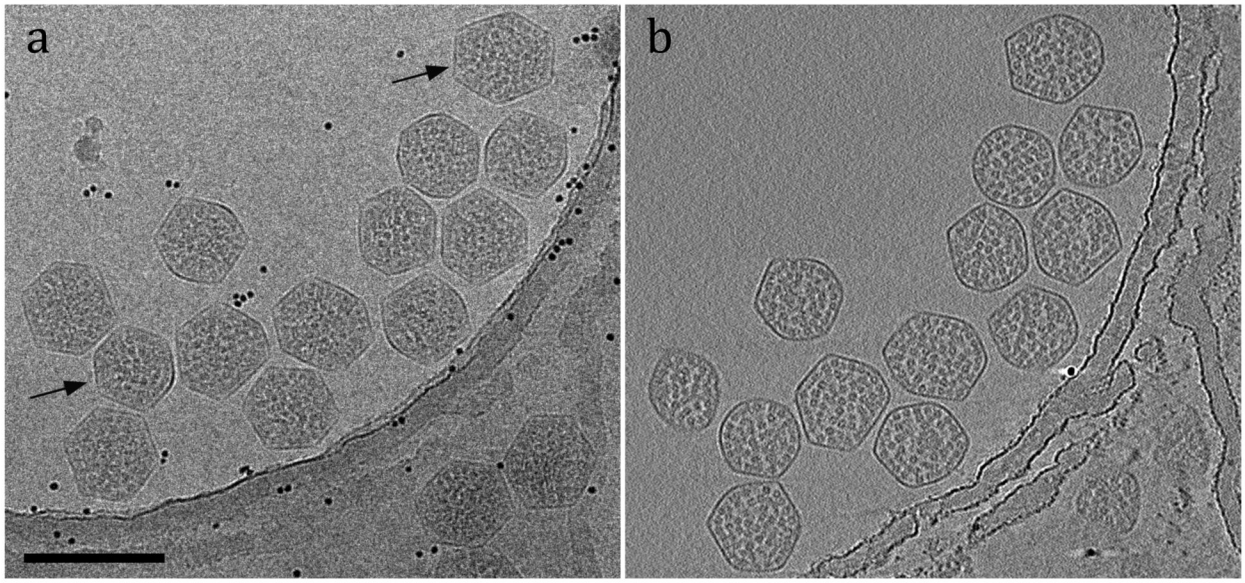

Figure 8.
Carboxysomes purified from *H. neapolitanus*: a) zero tilt image; b) 4.6 nm slice through tomographic reconstruction. Black arrows indicate different sizes of carboxysomes. Scale bar is 200 nm.

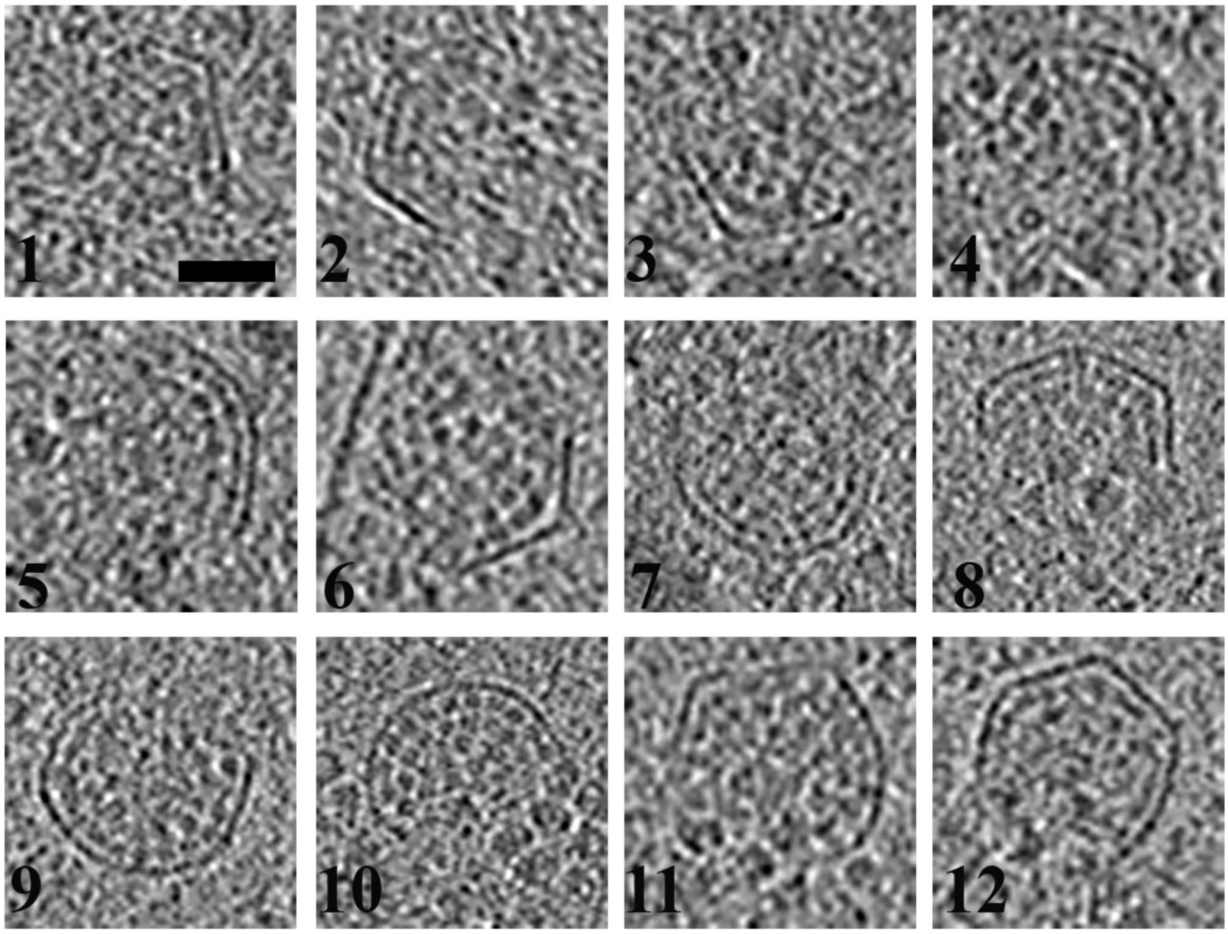

Figure 9.
Partial carboxysomes. The figure is organized such that more complete carboxysomes are at the bottom. Note the variability of partial carboxysome shapes, ranging from sharp vertices (e.g. panels 2, 3, 6, 12) to smooth, rounded surfaces (e.g. panels 4, 7, 9, 10), and that putative RuBisCOs pack within the interior as the shell forms. Scale bar is 50 nm.

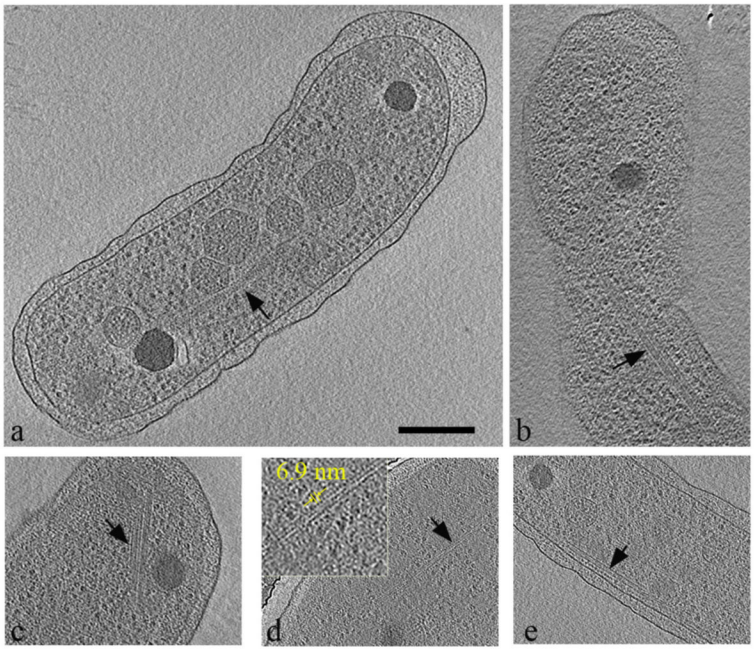

Figure 10.
Filament-like structures: a) *H. neapolitanus* cell showing a twisted filament associated with carboxysomes; b) parallel bundle in *H. neapolitanus*; c) parallel bundle in *T. intermedia*; d) parallel bundle in *H. neapolitanus* (inset shows periodicity measurement); e) parallel bundle in *H. neapolitanus* near the inner membrane. Note the linear arrangement of possible RuBisCOs between the bundle and the membrane. Scale bar is 200 nm.